

Use of superheated liquid in neutron detection*

S. C. Roy[†] and B. Roy

Department of Physics, Bose Institute, Kolkata 700 009, India

Detectors based on emulsions of superheated liquid drops in visco-elastic gels or soft polymers are being used for neutron detection, neutron dosimetry and neutron spectrometry for over two decades. When exposed to energetic radiation, superheated drops are nucleated to vapour bubbles due to the energy deposited in the liquid by the radiation while passing through the emulsion. Rate of nucleation was measured either using a passive device which requires no power source, or an active device which counts each drop nucleation electronically. Although the present article focuses mainly on the application of the superheated liquid in neutron detection, neutron dosimetry and neutron spectrometry, the basic principle of nucleation, measuring devices and methods have also been presented. Recent works on the use of superheated liquid in detecting gamma and other high Z radiation are also mentioned.

SUPERHEATED liquid has recently been used extensively as a radiation detector, and its superiority as a neutron detector compared to other conventional neutron detectors has already been established. Application of superheated liquid in radiation detection dates back to the time of the bubble chamber invented by Glaser; the invention earned him the Nobel Prize in 1960. In the bubble chamber, as an energetic particle passes through a suitable liquid kept in a huge chamber, pressure in the chamber is suddenly reduced to make the liquid superheated instantaneously, and the particle produces bubbles along its path. The trajectory of charged particles is then photographed and analysed. Since the boiling initiated at any point of the chamber eventually consumes the whole liquid, re-pressurization is required every time after detection of a particle and before detecting the next energetic radiation. Even the fastest bubble chamber does not work beyond about 20 cycles per second. The use of a superheated liquid in a more convenient form of radiation detector, known as the superheated drop detector (SDD), was first reported by Apfel¹ in 1979. In SDD, the whole liquid is dispersed homogeneously in the form of minute droplets in a gel-like medium. As an energetic particle passes through the detector, the liquid drops which interact with the radiation vapourize keeping other drops un-

affected and therefore the re-pressurization procedure required in the bubble chamber is not needed. In a sense, SDD is a continuously sensitive miniature bubble chamber. A similar device known as bubble detector (BD) was developed by Ing, in which superheated drops are homogeneously distributed in a rigid polymer matrix². In BD, vapour bubbles remain trapped inside the polymer. SDD is the trade name of superheated drop detector manufactured by Apfel Enterprises Inc., USA and BD is the trade name of the bubble detector manufactured by Bubble Technology Industries Inc., Canada. However, in recent years, 'superheated emulsion' is the common denomination adopted by the International Commission on Radiation Units and Measurements (ICRU) and by the International Organization for Standardization (ISO) to indicate any kind of detector using superheated drops, including SDD and BD.

Extensive research to develop this detector in a form suitable for laboratory and field experiments with repeatable results, carried out in the last two decades, established this device as a useful neutron detector to the extent that it has been included even in a graduate student textbook³. Within 20 years of its invention, superheated emulsions have made their place in almost all branches of radiation physics⁴, including nuclear physics, health physics, medical physics, space physics and high energy physics. Incidentally, this technology has been introduced by one of the authors (S.C.R.) in India and subsequently transferred to two national laboratories in the country. To the best of our knowledge, work using this detector is in progress in one of the defence research institutes and two atomic energy laboratories in India. In the present article, we primarily focus on the use of superheated emulsion in neutron detection, neutron dosimetry and neutron spectrometry, but its potential applicability for detection of other radiation will not be excluded.

Superheated liquid

Any liquid maintaining its liquid state at a temperature above its boiling temperature is called a superheated liquid. The typical phase diagram of a substance is shown in Figure 1, where point c is ordinarily in a pure vapour state. But if the state c maintains its liquid state at that pressure and temperature, we will call this a superheated state. As shown in Figure 1, the state c can be reached by

*The authors dedicate this article in memory of Robert E. Apfel, Yale University.

[†]For correspondence. (e-mail: scroy@bosemain.boseinst.ac.in)

slowly increasing the temperature (isobaric heating) from the liquid state *b* or by reducing the pressure (isothermal decompression), starting from the liquid state *d*. The degree of superheat can be defined as the difference in temperature of a liquid at a temperature higher than its boiling point and the boiling point of the liquid at a given pressure (the difference *fc* in Figure 1); or at given temperature, it is the difference in vapour pressure of the liquid in the superheated state and the equilibrium vapour pressure at that temperature (*gc* in Figure 1). The degree of superheat may be expressed in temperature or pressure scale.

The superheated state is a metastable state of the liquid, since the system is in a relative minimum energy state and not in its absolute minimum. The state is stable with respect to small perturbations (except at a temperature close to critical temperature) but unstable to larger disturbances and moves to a more stable equilibrium state (vapour). Disturbances are often the consequences of thermal motion and therefore the state depends on temperature. This could be well understood if the liquid–vapour phase diagram is represented in pressure–volume space, as shown in Figure 2. If a liquid is expanded beyond the point *B* of the *P*–*V* diagram, under special conditions it will follow the line *BC*. Along this line, the system is not in stable equilibrium; it is in a metastable state and a very small perturbation will change the system to the stable state represented by the line *BD*. But if there are no such disturbances, the liquid will remain as a liquid along this metastable equilibrium line⁵.

As shown in Figure 2, the liquid cannot be superheated by lowering the pressure (*P*) of the liquid beyond the point *C*, which is the minimum of the metastable superheated state at a given temperature. The lowest pressure represented by the point *C* is the maximum limit of superheat at a constant temperature. Such a minimum point is on the border between the metastable and the unstable

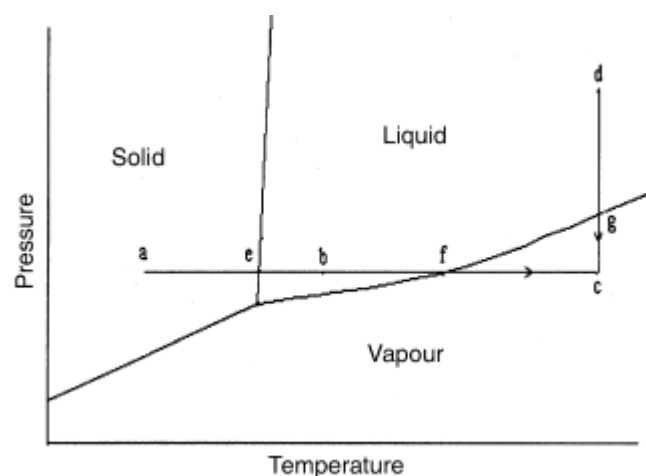


Figure 1. Typical phase diagram of a substance in solid, liquid and vapour phases.

liquid, which is known as the spinodal curve⁶. It is clear from Figure 2 that as temperature increases, depth of the metastable state decreases and vanishes at the critical temperature. This is the reason that although the theoretical upper limit of superheat is the critical temperature, one cannot reach this theoretical limit in practice since a very small thermal fluctuation is enough to overcome this energy barrier (as will be explained later in the text). At constant pressure, the limit of superheat is the maximum temperature below the critical point that a liquid can sustain without undergoing a phase transition (boiling).

In order to obtain a liquid in the superheated state, the liquid must be taken in a ‘perfectly smooth’ container and the liquid must not contain any impurities, air bubbles or gas pockets. The presence of any kind of discontinuity will act as a heterogeneous nucleation site which will facilitate the phase transition to the vapour state. Two types of nucleation are generally observed – homogeneous and heterogeneous. Nucleation in the bulk of the liquid is called ‘homogeneous nucleation’, and when the nucleation occurs at an interface such as solid–liquid, liquid–liquid or liquid–gas, it is called ‘heterogeneous nucleation’. Normal boiling, which we experience everyday, is an example of heterogeneous nucleation and this occurs at a temperature much below the homogeneous nucleation temperature. Liquids commonly used in preparing superheated emulsion are low boiling-point refrigerant liquids. Their chemical formulae and some physical properties are listed in Table 1.

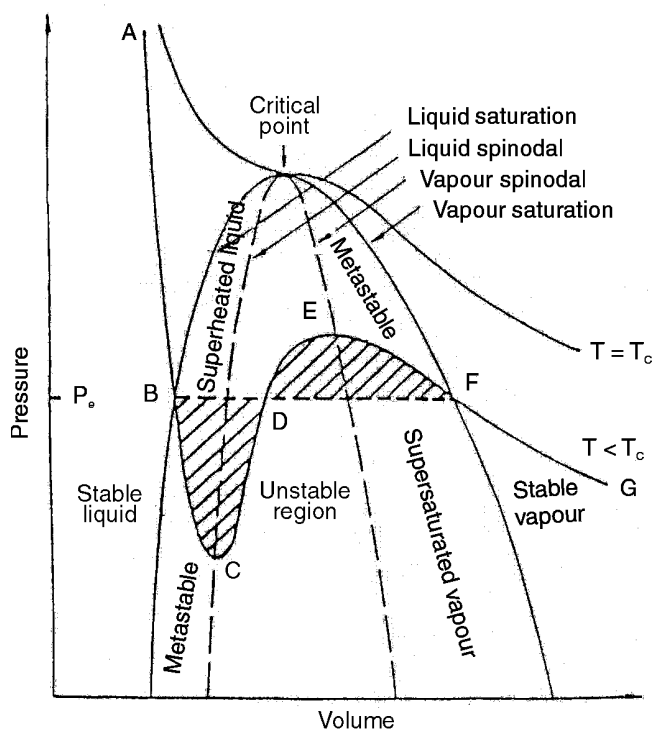


Figure 2. Schematic representation of pressure–volume isotherm for a pure liquid.

Table 1. Physical properties of some liquids used in superheated emulsions at 25°C

Liquid	R-12	R-21	R-22	R-115	R-114
Chemical formula	CCl ₂ F ₂	CHCl ₂ F	CHClF ₂	C ₂ ClF ₅	C ₂ Cl ₂ F ₄
Molecular weight	120.91	102.92	80.47	154.47	170.93
Boiling point (<i>T_b</i>) (°C)	-29.79	8.92	-40.75	-38.7	3.77
Surface tension (<i>g</i>) (dyn/cm)	9	18	8	5	13
Density (<i>ρ</i>) (g/cc)	1.293	1.354	1.175	1.291	1.456

In R-12...R-114, R stands for refrigerant liquid and 12...114 are the accepted representations of chemical formulae of liquids as found in the *CRC Handbook*, e.g. if a liquid is represented as R-xyz, then its chemical formula can be obtained as C_{x+1}H_{y-1}F_zCl_k, where $k = 2x - y - z + 5$.

'Superheated emulsion' is a generic name of any kind of radiation detector using superheated liquid drops. These include superheated drop detectors and bubble detectors available commercially. In addition, a few laboratories, including Bose Institute, Kolkata, prepare their own superheated emulsions and use them to characterize the properties of various liquids and their sensitivity to different energetic radiations. The basic requirement in preparing all such detectors is to hold the superheated drops in another immiscible liquid, which is closest to a 'perfectly smooth' container for all practical purposes. The method usually used in preparing superheated emulsions is isothermal decompression, which has been explained earlier.

Basic principle of nucleation

The word 'nucleation', in this context, means the formation of a nucleus of a new phase. The change from a metastable to a stable state occurs as a result of fluctuations in a homogeneous medium by forming a nucleus of a new phase. The energetically unfavourable process of creation of an interface has the result that when the nucleus is of a size less than a certain critical size, it is unstable and disappears by the action of surface tension. Only nuclei whose sizes are greater than the critical size are stable and grow very fast to the observable size⁷. Similarly, nucleation in the superheated state starts with the formation of a critical-sized vapour embryo. Homogeneous nucleation in this superheated state can be observed by the radiation interactions of ions, charged particles, neutrons, photons, etc. and also by large-scale density fluctuations at the molecular level. The existence of an energy barrier against nucleation arises because the interface between the liquid-vapour phases has a finite energy per unit area which is the surface tension of the liquid⁸. The free energy required to form a spherical vapour bubble of radius *r* in a liquid, was first given by Gibbs⁹ using classical thermodynamics as

$$G = 4\pi r^2 g(T) - (4\pi/3)r^3(p_v - p_o), \quad (1)$$

where *g*(*T*) is the surface tension (liquid-vapour interfacial tension) of the liquid at a temperature *T*, and *p_v* is the

equilibrium vapour pressure of the superheated liquid and *p_o* the ambient pressure. The pressure difference (*p_v*-*p_o*), often referred to as ΔP , is the degree of superheat of the liquid at a temperature *T*. The first term is the surface energy term which is required to create the surface of a vapour bubble of radius *r* against the force of surface tension at the interface. The second term is the volume energy term and it is required to produce the volume of a bubble of radius *r*. The nature of variation of *G* with radius of the bubble at different temperatures is shown in Figure 3. It can be seen from Figure 3 that the free energy increases with *r*, reaches a maximum and then decreases. The radius *r* at which *G* reaches a maximum is known as the critical radius. It is also to be noted that the height of the energy barrier decreases with increasing temperature and vanishes at *T* = *T_c*. This is the reason that, at a temperature close to *T_c*, any small perturbation such as thermal fluctuation may cause vapourization, and the critical temperature cannot be reached in practice.

G reaches its maximum at

$$r = 2g(T)/(p_v - p_o) = r_c, \quad (2)$$

and *r_c* is called the critical radius. When a bubble grows to the size of the critical radius, it becomes thermodynamically unstable and grows very fast till the entire liquid droplet vapourizes. Therefore, the nucleation will be possible only when the size of the bubble reaches the critical size *r_c*.

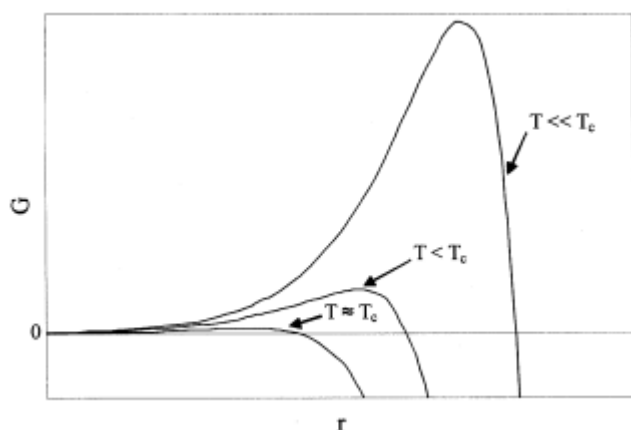
The minimum amount of energy (*W*) needed to form a vapour bubble of critical size *r_c* can be obtained by putting *r* = *r_c* in eq. (1), and is given by

$$W = 16\pi g^3(T)/3(p_v - p_o)^2. \quad (3)$$

Therefore, for nucleation to occur, at least this amount of energy is to be deposited within the liquid. Since the degree of superheat (*p_v*-*p_o*) increases and *g*(*T*) decreases with increase in temperature, the minimum energy (*W*) required for vapour nucleation decreases with increase in temperature. Thus *W*, the threshold energy for nucleation depends on the type and the temperature of the liquid. Table 2 shows how *W* varies with change in degree of

Table 2. Properties of some superheated liquids related with radiation detection when operated at atmospheric pressure and at 25°C

	R-115	R-12	C-318	R-114
Boiling point T_b (°C)	-38.7	-29.79	-5.8	3.77
Vapour pressure P_v (atmos.)	8.91	6.38	3.01	2.10
Degree of superheat ($p_v - p_o$) (atmos.)	7.91	5.38	2.01	1.10
Degree of superheat ($T - T_b$) (°C)	63.7	54.79	30.8	21.23
Critical radius r_c (cm)	1.3×10^{-6}	3.1×10^{-6}	7.8×10^{-6}	2.3×10^{-5}
W (keV) (eq. (3))	0.0203	0.227	1.25	48.35
Nature of radiation detected	Light ions, neutrons and photons	Heavy ions, neutrons > thermal	Heavy ions, neutrons > 2 MeV	Heavy ions, neutrons > 8 MeV


Figure 3. Variation of G with radius (r) of bubble at different temperatures.

superheat and how this property helps to detect low energy-transfer radiations (such as X-rays and gamma rays) as well as low energy neutrons with increasing degree of superheat.

Limit of superheat

One may now ask a question: what is the maximum degree of superheat that a liquid can attain or how high can the temperature of a liquid be raised without boiling? The theoretical upper limit of superheat is the critical temperature (T_c) of the liquid, since above this temperature the liquid phase can no longer exist. However, critical temperature cannot be reached in practice, although there is a maximum attainable temperature for a given liquid without boiling, known as the 'limit of superheat' (T_{sl}) of the liquid. It is interesting to see how close one can reach to the theoretical upper limit experimentally.

The limit of superheat can be estimated either from the thermodynamic stability theory or from the analysis of the dynamics of formation of the critical-sized vapour embryos (statistical mechanical theory). Using van der Waals equation of state, one may calculate the maximum limit of superheat as

$$T_{sl} = 27T_c/32. \quad (4)$$

An empirical relationship valid for most of the organic liquids is also available¹⁰ as given by

$$T_{sl} = T_c[0.11(P/P_c) + 0.89], \quad (5)$$

where P_c is the critical pressure and P is the ambient pressure. The statistical mechanical theory predicts the rate of formation of critical-sized vapour embryos per unit volume (J) as given by

$$J = Nf \exp(-W/kT), \quad (6)$$

where N is the number density of molecules in the superheated liquid and a J value of 10^6 nucleation/ m^3s is often used to define the limit of superheat temperature, W is the minimum thermodynamic energy required for vapour formation (eq. (3)), k is the Boltzmann constant, f is a frequency factor which in general is of the order of $10^{11} s^{-1}$ and T is the temperature in Kelvin.

An answer to the question posed at the beginning of this section has been provided recently by Das *et al.*¹¹. Drops of superheated liquid (R-114, R-12 and R-22) are suspended in degassed, 'clean' visco-elastic gel. This avoids heterogeneous nucleation sites and also minimizes nucleation at the solid-liquid interface. A vial containing the superheated sample was placed on top of a thin layer of gel taken in a beaker. Some extra gel was placed on top of the superheated sample to accommodate a thermometer without affecting the superheated drops. The beaker was then placed on a piezoelectric transducer with a coupling gel. A schematic diagram of the experimental set-up is shown in Figure 4. The vial was wrapped with a heating coil and temperature of the sample was raised slowly using a temperature controller until nucleation occurred. Drop-nucleation was sensed by the piezoelectric transducer and the electric signal sent out of it was then amplified and fed to a multichannel analyser operating in a multichannel scaling mode. The drop vapourization rate (dN/dt) was recorded continuously with temperature (N being the number of drops present at any instant of time t). Ideally, it is expected that at all temperatures below the limit of superheat, $(1/N)(dN/dt)$ is zero and it shoots up to 1 at the limit of superheat.

Table 3. Comparison of predicted limit of superheat with those from other experiments

Liquid	Critical temperature (K)	Experimental T_{sl} (K)		Reduced limit of superheat [$T_{sl}(K)/T_c(K)$]				
		Das <i>et al.</i> ¹¹	Reid ¹⁰	Predicted			Experimental	
				Eq. (4)	Eq. (5)	Eq. (6)	Das <i>et al.</i> ¹¹	Others ^{10,13}
R-12 (CCl ₂ F ₂)	384.5	353.0	345.0	0.84	0.89	0.90	0.92	0.90 (ref. 10)
R-114 (C ₂ Cl ₂ F ₄)	418.7	393.5	375.0	0.84	0.89	0.91	0.94	0.90 (ref. 10)
R-22 (CHClF ₂)	369.0	330.5	327.0	0.84	0.89	0.89	0.89	0.89 (ref. 10) 0.89 (ref. 13)

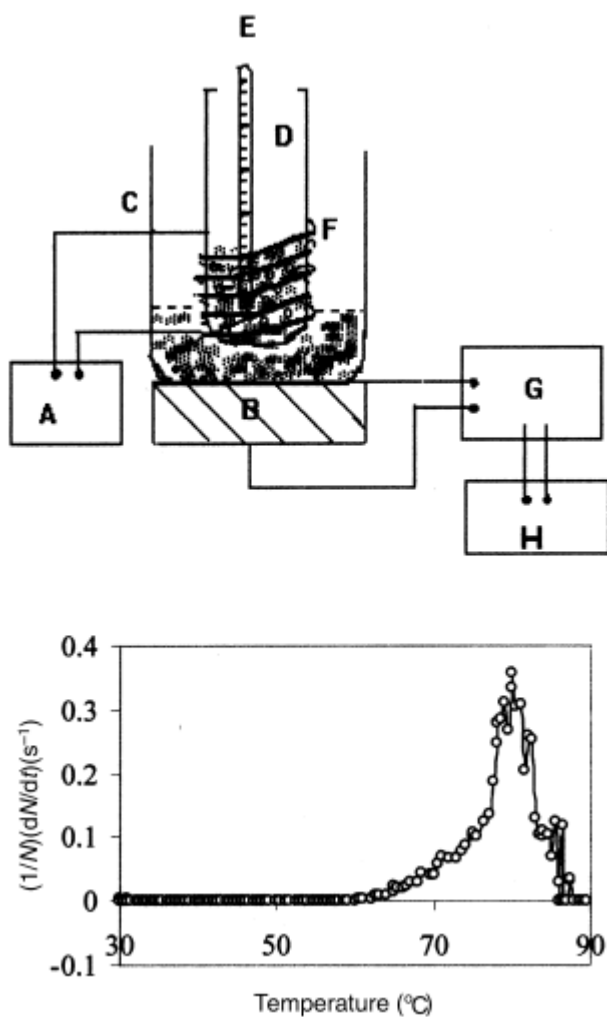


Figure 4. *a*, Schematic diagram of the experimental arrangement for determining limit of superheat. A, autotransformer; B, piezoelectric transducer; C, glass beaker; D, glass vial containing sample; E, thermometer; F, heating coil; G, drop counter; H, multichannel analyser. *b*, Variation of normalized nucleation rate with temperature for R-12, showing the sudden increase of rate of nucleation at limiting temperature.

As a representative example, the variation of $(1/N)(dN/dt)$ with temperature for R-12 is shown in Figure 4. A comparison of the observed limit of superheat with other

experimental results is presented in Table 3. The reduced limit of superheat defined as (T_{sl}/T_c) for those liquids is also presented along with theoretically predicted values and other experimental results.

Experimental values of T_{sl} reported so far are less than the predicted limit of superheat in some liquids¹² and larger in some cases¹⁰. The present results¹¹ exceeded the predicted limit of superheat and those from other experiments. The experimental values, prior to this measurement, reveal that the reduced limit of superheat (defined as $T_{sl}(K)/T_c(K)$) of only 14 out of 56 liquids studied by Avedisian¹³ hardly exceeded 90%. By holding superheated samples in a visco-elastic gel in the experiment of Das *et al.*¹¹, chances of heterogeneous nucleation were substantially reduced. Observing 'pure' homogeneous nucleation without any chance of heterogeneous nucleation is difficult if not impossible to achieve. In addition, the nucleation was recorded more precisely by Das *et al.*¹¹ using digital electronics for the first time. It is to be noted in this connection that all theoretical predictions are approximate and therefore this experiment also indicates the need for improved calculations.

Radiation-induced nucleation

In radiation-induced nucleation, the minimum energy needed for nucleation is supplied by the energetic radiation passing through the liquid. Charged particles, while passing through matter, lose energy by electromagnetic interactions. Such loss of energy of charged particles represented by the linear energy transfer (LET) or (dE/dx) , depends on the nature of the particle, its energy and the material through which it passes. Therefore, LET of the incident particle plays a major role in nucleation. Radiation-induced nucleation is a complex process covering a length scale of about twelve orders of magnitude (the process starts with nuclear interactions and ends with macroscopic vapour bubble formation) and it is, therefore, difficult to develop a complete theory of radiation-induced nucleation. For uncharged particles like neutrons or gamma rays, the energy deposition takes place by sec-

ondary particles produced due to the interaction of neutrons and gamma rays with the liquid medium.

Glaser¹⁴, in explaining the bubbles formed in a bubble chamber by charged particles, originally suggested that the formation of bubbles might be associated with the development of electrostatic forces produced by the charges induced by ionization and is related to the production of free electrons (**d** rays). However, the approximate theory proposed by Seitz¹⁵, known as the 'thermal spike' theory, is considered to be more or less accurate in describing the general mechanism of nucleation. According to this model, mechanism of bubble formation depends upon the production of highly localized hot regions or 'temperature spikes' within the liquid, which literally explode into bubbles larger than the critical size that grow through evaporation of the superheated liquid.

A more accurate expression of the minimum energy required to form a critical bubble has been proposed by Bell *et al.*¹⁶ on consideration of dynamic factors such as viscosity and is given by

$$E_m = W + H + E_{\text{wall}} + F. \quad (7)$$

Here H is the vapourization energy which is considered to be taken from the ambient liquid and is given by $(4\pi/3)r_c^3 \rho_v h_{\text{fg}}$, where ρ_v is the vapour density and h_{fg} is the latent heat of vapourization. The third term is the kinetic energy imparted to the liquid by the motion of the vapour wall. The term F represents the energy imparted to the liquid during the growth of the bubble by the action of the viscous forces. It has been found that the contribution of the third and fourth terms of the above equation is negligible. The complete and accurate dynamic theory of radiation-induced nucleation in superheated liquids has been proposed by Sun *et al.*¹⁷. Apart from a few assumptions considered in developing the model, a major problem of the dynamic theory is the requirement of prohibitive computation time for each calculation and from this point of view, approximate 'thermal spike' theory is commonly used in analysing experimental observations.

Neutron-induced nucleation

Neutrons interact with the nuclei of the interacting material basically by three processes: (a) nuclear reactions, (b) nuclear elastic scattering, and (c) nuclear inelastic scattering. Nuclear reactions are important for thermal and 'slow' neutrons, while scattering is important for fast neutrons. In order that nucleation occurs, the process by which maximum amount of energy is transferred to the interacting material is of primary importance. It is known that elastic scattering could transfer the maximum amount of energy to the target nuclei and therefore, we essentially consider elastic scattering as a major mecha-

nism in nucleation of superheated drops in case of fast neutrons.

If a neutron of energy E_n interacts with a nucleus of atomic weight A , the energy E_i transferred to the i th nucleus from the neutron through elastic scattering is given by

$$E_i = 4AE_n \cos^2 \mathbf{q} (A + 1)^2, \quad (8)$$

where \mathbf{q} is the recoil angle. Equation (8) shows that the maximum energy that can be transferred to the nucleus from the neutron is through the elastic head-on collision and is given by,

$$E_i = 4AE_n / (A + 1)^2. \quad (9)$$

After receiving this energy, the nucleus of the atom of the superheated liquid drop is usually scattered-off from its atom and moves through the liquid, losing its energy through Coulombic interactions until it comes to rest. As can be seen from eq. (9), for a given neutron energy different nuclei of the liquid will receive different amounts of energy depending on their atomic weight. These nuclei deposit different amounts of energy in the liquid determined by what is known as LET or (dE/dx) in the liquid. Figure 5 shows the linear energy transfer of different nuclei of the liquid when neutrons of different energy interact with the liquid R-12, which contains carbon (C), chlorine (Cl) and fluorine (F). The energy deposited by the recoil ions (E_c) within a distance L along the ion track must exceed the minimum thermodynamical energy W

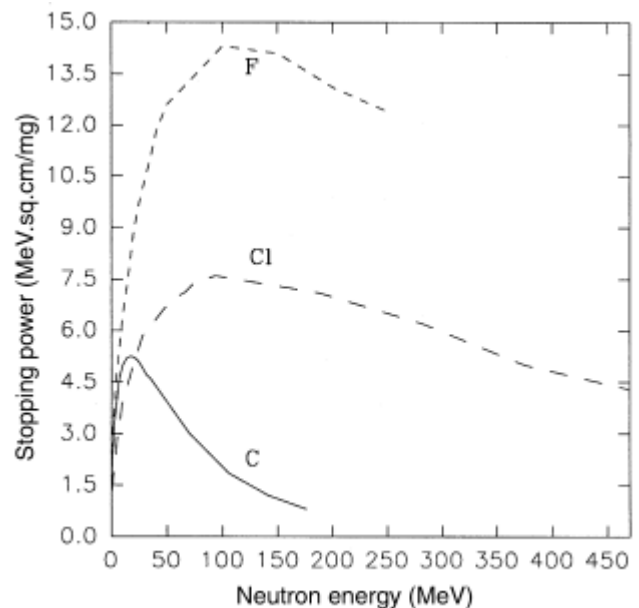


Figure 5. Variation in dE/dx of C, Cl and F in R-12 with neutron energy.

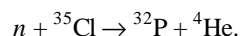
needed for nucleation to occur. It has been argued by Apfel *et al.*¹⁸ that the length corresponding to about twice the critical radius r_c plays a significant role in superheated drop nucleation. Mathematically,

$$E_c = L(dE/dx) = kr_c(dE/dx) \geq W, \quad (10)$$

when L is expressed in units of r_c .

Nuclear reactions play a major role in the detection of low-energy neutrons, as is evident from the observed sensitivity of R-12 (CCl_2F_2) to thermal neutrons at room temperature¹⁸⁻²⁰. The calculated minimum energy (W) needed to nucleate R-12 drops at room temperature is 0.227 keV, while the energy of the thermal neutrons are about three orders of magnitude less than W . It has been proposed that the thermal neutron sensitivity of R-12 is due to the following nuclear reactions:

$n + {}^{35}\text{Cl} \rightarrow {}^{35}\text{S} + p + 615 \text{ keV}$ [this energy is distributed between proton (598 keV) and the sulphur ion (17 keV)],



However, the probability (cross-section) of the first reaction is about four orders of magnitude greater than the second one, and therefore it is assumed that the thermal neutron sensitivity of R-12 at room temperature is due to the first reaction. The proton of energy 598 keV deposits only a small fraction of its energy in the critical bubble. The sulphur ion deposits its entire 17 keV in a range that is physically less than the critical radius which causes the nucleation.

Detection of nucleation

When superheated emulsions are exposed to energetic radiation, the superheated drops interacting with the radiation nucleate (change to vapour bubbles). The viscoelastic property of the holding medium prevents other neighbouring drops to nucleate. For a given sample and a specific kind of radiation, the number of drops nucleated is proportional to the number of energetic particles incident on it. Thus by measuring the number of nucleations occurring in a given time, one can find the flux of incident particles and the dose. There are two means by which one can measure the number of nucleations: one is by using what are known as active devices and the other by what are known as passive devices. The passive device does not require any power source and is more suitable for personnel dosimetry and medical physics applications, the active device is used for counting each drop nucleation electronically.

A simple passive device is that of counting vapour bubbles visually. In fact, there are instruments available commercially (Neutrometer S marketed by Apfel Enterprises

Inc, USA and Bubble Detector marketed by Bubble Technology Industries Inc, Canada) in which bubbles are counted visually. However, this method of counting bubbles is reasonable only when the incoming flux of radiation is small or nucleation rates is very low. For higher nucleation rates, counting of bubbles is done optically by a digital scanner or by measuring the volume of vapour formed due to nucleation.

An apparatus to measure more accurately the amount of vapour volume formed has been developed indigenously by Das *et al.*²¹. A schematic diagram of the apparatus is shown in Figure 6. In this device, a glass vial containing superheated drops is connected to a horizontal glass tube containing a small coloured water column (used as a marker) which is placed along a graduated scale. Vapour formed due to drop nucleation pushes the water marker along the glass tube. The displacement of the water column is directly related to the nucleated volume. In this set-up²¹, a glass tube of 1 m length has been used in order to keep the instrument to a reasonable size. With this set-up, a neutron dose as small as 0.1 μSv could be measured. The sensitivity of the apparatus could be increased, in principle, by choosing a glass tube of smaller diameter. In addition to its superior sensitivity, this device, unlike other existing passive devices, is capable of taking real time measurement by placing the detector vial in the radiation area, while placing the measuring apparatus in the control room.

In another passive device (Neutrometer HD, marketed by Apfel Enterprises Inc, USA), a 1 ml pipette with 0.1 ml resolution containing thick gel is attached to the vial containing superheated drops. As drops nucleate, the vapour formed pushes the gel along the pipette and gives a measure of the amount of radiation received. In Neutrometer HD, the scale of the pipette is calibrated against neutron dose and is used as a neutron dosimeter.

The active device counts the number of drops nucleated instantaneously by electronic means and was first developed by Apfel and Roy²². The glass vial containing the superheated drops was placed on the top of a piezoelectric transducer. Every time a drop nucleates, the pressure pulse produced due to the release of pressure is sensed by the transducer and an electric signal is produced. This electric signal is then amplified, digitized and counted. Further improvement of the device has been made in our laboratory and has been reported in one of our recent publications^{4,23}, a block diagram of which is presented in Figure 7.

Superheated drops are suspended in the gel without physically touching each other and they nucleate in a random manner independent of each other. Under such conditions, it can be shown that the number of drops would decay exponentially with a time constant τ (lifetime). If a vial containing superheated drops is kept in a neutron field such that neutrons of flux ϕ are incident on the drops of total volume V , liquid density ρ and mole-

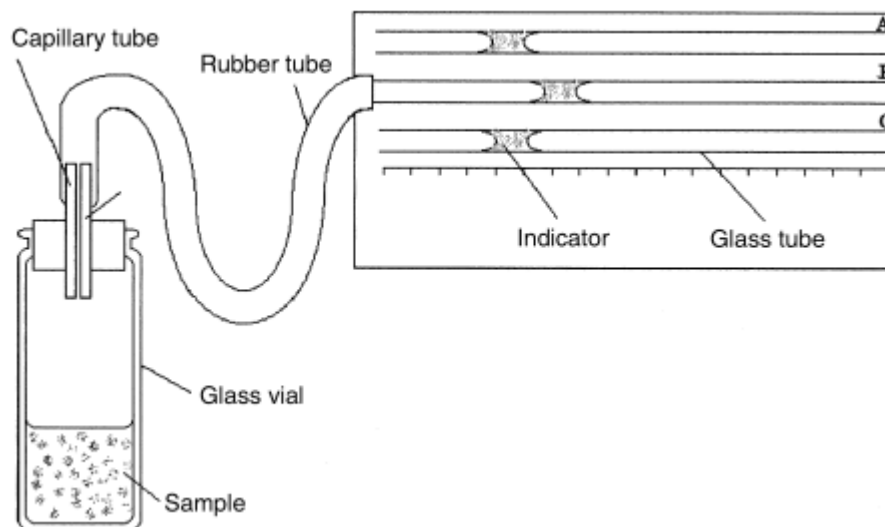


Figure 6. Schematic diagram of a passive device used to measure vapour volume formed due to radiation-induced nucleation.

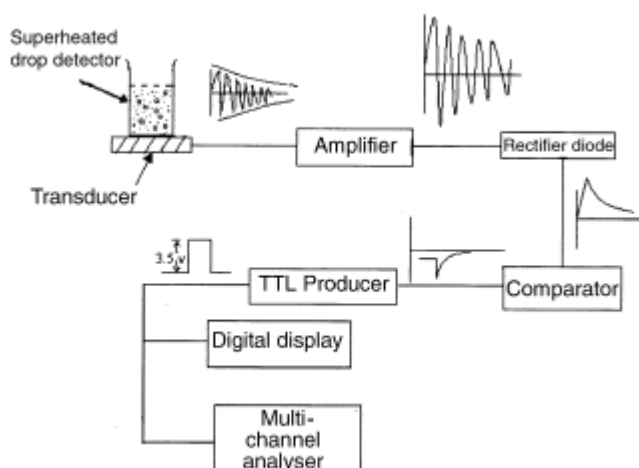


Figure 7. Schematic diagram of active device used to count radiation-induced nucleation in superheated emulsion.

cular weight M , the initial rate of volume of vapour formed is given by

$$dV/dt = V \mathbf{y} N_A \mathbf{r} \mathbf{h} \Sigma n_i \mathbf{s} / M, \quad (11)$$

where N_A is the Avogadro number, d is the average droplet volume, n_i is the number of nuclei of the i th element of the molecule whose neutron-nucleus cross-section is \mathbf{s} , and \mathbf{h} is the efficiency of neutron detection.

In the air-displacement passive device mentioned above, change in position (h) of the water column along the glass tube due to nucleation of drops by neutrons could be measured as a function of time. So, the rate of increase of mass of vapour during nucleation should be

equivalent to the rate of decrease of the mass of the superheated liquid. Therefore, one can write

$$\mathbf{r} A (dh/dt) = -\mathbf{r}_v (dV/dt) = -\mathbf{r}_v \mathbf{y} N_A \mathbf{r} \mathbf{h} \Sigma n_i \mathbf{s} / M, \quad (12)$$

where A is the cross-sectional area of the horizontal tube, \mathbf{r}_v is the density of vapour of the liquid and V is the total volume of the superheated drops existing at time t . A typical graph representing variation of vapour volume with time for R-12 drops is shown in Figure 8.

Integrating and solving the above equation, one may obtain

$$(hA/m) = a[1 - \exp\{-b(t-t_0)\}], \quad (13)$$

where

$$a = V_0 \mathbf{r} / (\mathbf{r}_v m), \text{ and } b = (1/t) = \mathbf{y} N_A \mathbf{r} \mathbf{h} \Sigma n_i \mathbf{s} / M. \quad (14)$$

Here hA/m is the volume of accumulated vapour in time t per unit mass of the superheated sample containing superheated drops and gel. By fitting eq. (13) for different values of h and t , values of a , b and t_0 are obtained. The slope of this curve at initial time t_0 is a measure of the initial nucleation rate at $t = t_0$ and can be obtained from eq. (13) as

$$[(d/dt)(hA/m)] = ab. \quad (15)$$

Since for a given sample of known volume of superheated drops a is known, b could be determined from the slope. From b , one can find the value of \mathbf{h} when all other quantities are known.

In the case of the active device, V will be replaced by N , the number of drops present at any instant of time t .

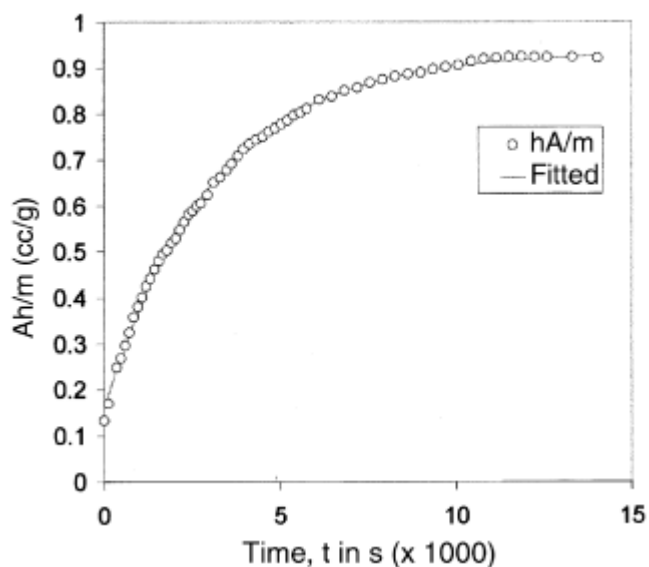


Figure 8. Variation of vapour volume formed per unit mass of superheated emulsion with time for R-12.

Superheated emulsion as neutron dosimeter

Historically, application of superheated emulsions started with the development of a neutron dosimeter^{24,25}. This was because of the fact that the dose-equivalent response of the available personnel dosimeters was inadequate to meet the requirements set by the International Commission of Radiological Protection (ICRP). Passive devices made of superheated emulsions are probably the only passive neutron dosimeters which meet the ICRP requirements when compared with other commonly used dosimeters such as TLD-albedo dosimeter or film dosimeter. In addition, unique properties such as its photon insensitivity, passive operation, tissue equivalent composition, isotropic response, small size, instant dose-reading capability and low cost make these detectors one of the most useful tools in neutron dosimetry.

The only disadvantage of this device is its temperature-dependent sensitivity. However, this could be compensated by using a low boiling point liquid²⁶ or thermally expansible material² on top of the sensitive emulsions kept in a sealed tube. The vapour tension of the liquid or the volume occupied by the expansible material increases with ambient temperature and the pressure it exerts on the detector compensates to a large extent the temperature dependence of the response. It has been found in one of the passive devices that the temperature sensitivity reduces from 5% change per degree Celsius to 1% per degree Celsius when temperature compensation method as described above was used. The performance characteristics of these personal dosimeters have been investigated extensively in terms of reproducibility and linearity of measurements, sensitivity to environmental conditions, mechanical stress, ageing, etc. It has been concluded that

the detectors could be used reliably over periods of time that actually exceed the manufacturer's specifications^{27,28}. This detector has also been included in the graduate student textbook on radiation detectors under the name 'superheated drop detector' and 'bubble (damage) detector'³.

The special properties that these dosimeters possess make them an ideal choice for application in radiotherapy using high-energy X-ray beams to assess the neutron dose. High-energy X-ray radiotherapy machines are known to generate neutrons by photo-disintegration or electron-disintegration of atomic nuclei in various components of the accelerator, treatment room, and also from the body of the patient. These contaminant neutrons expose the patient to an unwanted dose and also produce secondary radiation by neutron-capture reactions occurring in the body of the patient and in the accelerator. Medical accelerators producing photons with energies above 6–8 MeV are potential sources of unwanted neutrons. In fact, 1994 AAPM code of practice for radiotherapy accelerators recommends that 'for high energy machines with a nominal energy above 15 MeV, measurements should also be made of neutron leakage both inside and outside the room'.

Accurate measurement of neutron dose by conventional neutron dosimeters is impossible to achieve. The presence of extremely intense and pulsed primary photons masks measurement of neutron dose. The intensity of scattered photons produced by scattering of primary photons from the walls of the room, body of the patient, etc. is three to four orders of magnitude larger than the intensity of neutrons produced. Moreover, due to the complex nature of the neutron energy spectrum, use of conventional dosimeters which do not correspond well with the ICRP dose-equivalent curve over the entire range of neutron energy does not produce accurate results. Superheated emulsions, being photon insensitive and capable of producing dose-equivalent measurements directly without prior knowledge of the neutron energy spectrum, are a natural choice in this situation. Recent applications of superheated emulsions in measuring doses in phantoms in connection with radiation therapy using high-energy medical accelerator produced some interesting and useful results^{29,30}. The small size of the detector made possible the first *in vivo* measurement of neutron dose to patients³¹ while irradiating with high-energy X-ray beam.

Superheated emulsion as a neutron spectrometer

Application of superheated emulsion in neutron spectrometry utilizes the basic principle of radiation-induced nucleation in superheated liquid, i.e. threshold energy of nucleation decreases with increasing degree of superheat. Therefore, liquids with lower boiling points possess

higher degrees of superheat at a given ambient temperature (above their boiling points) and as the ambient temperature increases, the given liquid becomes more and more superheated. There exist, therefore, two distinct types of methodologies in the development of neutron spectrometer using superheated emulsions. In one, collection of superheated samples made of liquids with different boiling points is utilized³², while in the other, ambient temperature of the superheated sample is increased. d'Errico *et al.*^{33,34} used two liquids with different boiling points and the temperature of the liquids was set at four different values to obtain eight sets of threshold energy. Recently, Das *et al.*³⁵ used a single liquid and the temperature was varied continuously over a wide range. By controlling the temperature continuously one can, in principle, change the threshold neutron energy to any desired level and therefore can scan the neutron energy spectrum with better resolution. In the work of Das *et al.*^{35,36}, the relationship between the temperature and threshold neutron energy has been established using a novel method. Contrary to the conventional method of observing nucleation at different temperatures or for liquids with different boiling points using a monoenergetic neutron source, the basic principle of nucleation was used to determine the threshold energy–temperature relationship. Getting a monoenergetic neutron source of any energy of choice is difficult, and only a few establishments have these facilities. The present method eliminates the need for monoenergetic neutron sources of different energies for calibration.

In this article the neutron detection efficiency (\mathbf{h}) of the R-12 superheated drop sample exposed to Am–Be neutron source was measured at different temperatures using the passive device as described above. From the variation of \mathbf{h} with temperature of the detector, the derivative of efficiency ($d\mathbf{h}/dT$) was plotted against temperature. The resulting curve resembles the neutron energy spectrum of the neutron source. The temperature of the detector can be converted to the threshold energy of the incoming neutrons as given below.

As presented earlier, for a given neutron energy, different nuclei of the liquid receive different amount of energy, depending on their atomic weight, according to eq. (9). Also, they must have different LET or (dE/dx) in the superheated liquid. In case of the superheated liquid R-12 containing the nuclei C, Cl and F, (dE/dx) of all these ions corresponding to their energies has been determined and the average of (dE/dx) is calculated for determining the effective LET in the liquid. The variation of (dE/dx) of different ions with neutron energy has been presented in Figure 5.

The energy deposited over a specific length L along the ion track plays a significant role in nucleation. This length can be related to the critical radius r_c by the relation $L = kr_c$, where k is a constant. The energy deposited by the recoil ion (E_c) is given by eq. (10). For nucleation

to occur, this deposited energy should be at least equal to or greater than W . Therefore, in order to determine threshold,

$$W = E_c = kr_c(dE/dx), \quad (16)$$

or

$$W/r_c = k(dE/dx). \quad (17)$$

In this equation, the left hand side is a function of temperature and the right hand side is a function of the neutron energy via (dE/dx) of the recoil ion energy and therefore relates the temperature of the sample with the threshold neutron energy. This principle has been used to find the temperature threshold relation by finding the values of k that fit eq. (17). This method, therefore, does not require using monoenergetic neutrons of different energies to find the temperature–threshold energy relationship in a given liquid as done by d'Errico *et al.*^{33,34}. It is to be noted that in calculating this relationship only the elastic scattering of neutrons has been considered to be the mode of interaction in transferring energy to the nuclei. This is, in general, true for fast neutrons since maximum energy transfer is done through elastic scattering. For thermal and slow neutrons, where neutron-induced reactions predominate and energy transfer is mainly done by the reaction products, one has to consider all possible neutron-induced reactions and calculate the amount of energy transfer by the reaction products.

In another experiment, Das *et al.*^{37,38} studied, by the same passive device, the neutron energy spectrum of Am–Be neutron source using superheated drops of R-114 by varying its temperature almost continuously from 15 to 70°C. Variation of neutron detection efficiency (\mathbf{h}) as a function of temperature is represented in Figure 9. An integrated spectrum of the source is shown in Figure 9 and the solid line is the spline smoothing of the efficiency data at different temperatures. The uncertainties presented in Figure 9 are total experimental uncertainties of estimating \mathbf{h} . The derivative of efficiency with respect to temperature, which resembles the neutron energy spectrum of the neutron source is shown in Figure 10. The second peak appearing at higher temperature is due to the nucleation caused by gamma rays present in the Am–Be neutron source, as will be explained later in the text. For an optimum value of k , the temperature axis of Figure 10 has been converted to neutron energy and the resulting spectrum is fitted with the peak neutron energy of the Am–Be neutron spectrum. The best fit is obtained for $k = 0.1158$. Comparison of the threshold neutron energy (E_n) corresponding to each temperature obtained by Das *et al.*^{37,38}, with those obtained by d'Errico *et al.*^{33,39} and Apfel *et al.*¹⁸ using monochromatic neutron sources has been presented in Figure 11. The agreement between the results confirms the validity of the present method of estimating threshold neutron energy at different tem-

peratures. The neutron energy spectrum of Am-Be source obtained from this analysis is shown in Figure 12.

Recently, Apfel and d'Errico⁴⁰ have reported the development of a neutron spectrometer based on an active device of acoustic sensing of drop vapourization interfaced with a proportional-integral-derivative temperature controller. This is an automated process of measuring the neutron energy spectrum based on the active monitor for neutrons, called REMbrandt™, as the platform for controlling temperature on a SDD probe and for data acquisition.

This version of the spectrometer relies on eight thresholds only, but there is provision for extension to more temperature values.

Superheated emulsion in gamma ray detection

Though neutron dosimetry and neutron spectrometry using superheated drops have already been established, application of superheated drops in detection of photons

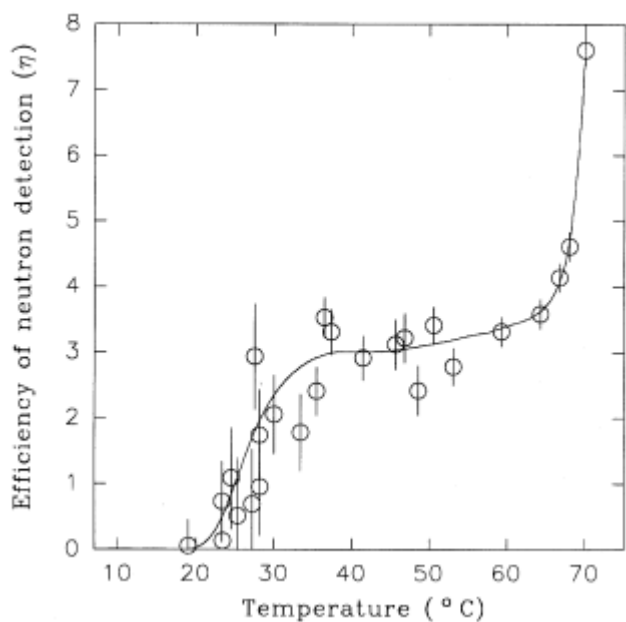


Figure 9. Variation of neutron detection efficiency with temperature for R-114.

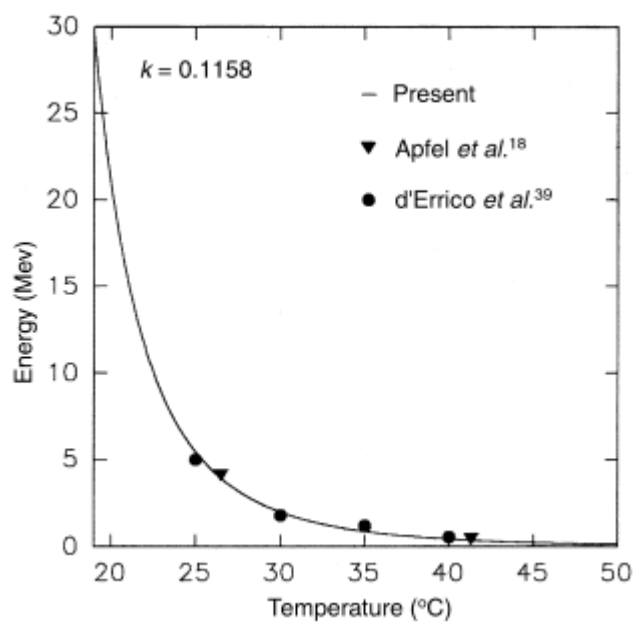


Figure 11. Variation of threshold neutron energy with temperature for R-114.

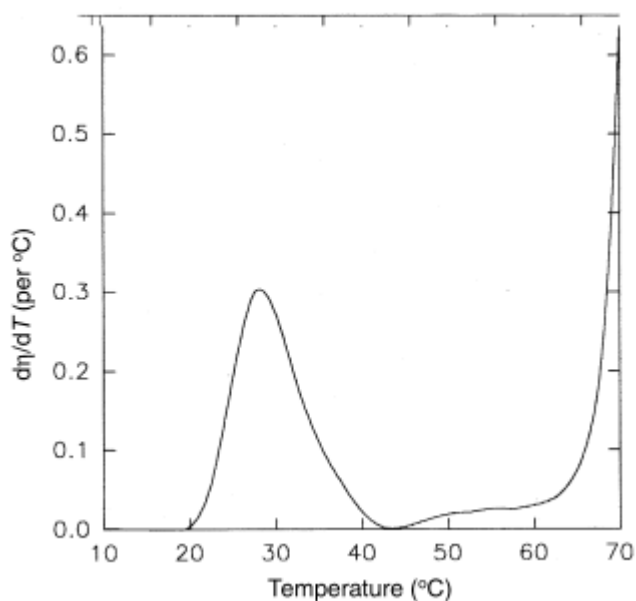


Figure 10. Variation of derivative of efficiency with temperature for R-114.

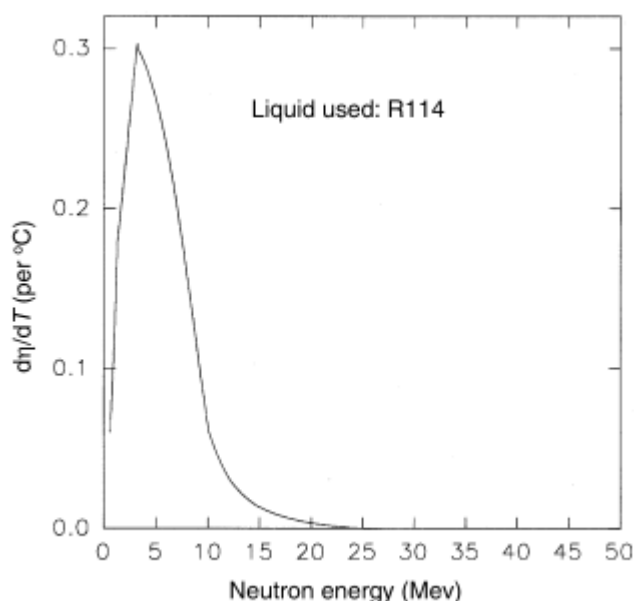


Figure 12. Neutron energy spectrum of Am-Be source obtained from experiment.

is still in its infancy. It has been found that moderately superheated emulsions being sensitive to neutrons at a given temperature, are yet insensitive to low-LET radiations like gamma rays and electrons. The reason is that these low-LET radiations cannot contribute sufficient energy required to nucleate, while neutrons can do so through the production of secondary charged particles having high LET values. Therefore, most of the moderately superheated liquids suitable for neutron detection at room temperature could detect photons only at higher temperatures when they are in a highly superheated state.

In a separate experiment using ^{241}Am gamma rays, we have observed that the rate of nucleation starts around 50°C in R-114 and reaches its maximum at about 70°C . This result confirms the steep rise in efficiency observed near 70°C in neutron spectrometry work (see Figure 9), which is due to the photons coming out of the Am–Be neutron source. It is known⁷ that the temperature at which all of R-114 drops will be nucleated without any external radiation source, known as the limit of superheat, is 120°C . Therefore, this steep rise in rate of nucleation near 70°C is due to the presence of gamma rays.

Some liquids sensitive to gamma rays at room temperature have been reported earlier^{23,32,41}. However, complete characterization of these detectors for applications as practical photon dosimeters is the recent focus of research.

d'Errico *et al.*⁴¹ suggested that a liquid becomes photon-sensitive at a temperature close to the midpoint between its boiling point and its critical temperature. According to d'Errico *et al.*⁴¹, superheated drops of R-12 (boiling point -29°C and critical temperature 111.5°C) will be photon-sensitive at about 41°C . However, Roy *et al.*⁴² demonstrated experimentally the sensitivity of R-12 detector to gamma rays at room temperature (25°C), when exposed to 59.54 keV photons. In another experiment, Roy *et al.*⁴³ have also observed that superheated drops of R-12 are sensitive to different energetic photons at different temperatures. Investigation by d'Errico *et al.*⁴¹ on the use of superheated liquids as suitable photon dosimeters shows great promise for the use of superheated emulsion in three-dimensional photon dosimetry. d'Errico³⁹ attempted a unified parametrization of the properties of superheated emulsions of light halocarbons, introducing a quantity called reduced superheat and defined as $s = (T - T_b)/(T_c - T_b)$. With this concept he claims to predict the 'macroscopic' features such as neutron detection thresholds, sensitization to thermal neutrons and to photons, and thermal limit of applicability.

d'Errico⁴⁴ suggested that the increase in photon sensitivity with increasing temperature above the threshold may be due to detection of clustered energy deposition events of decreasing size, which justifies the definition of nano dosimeters attributed to the superheated emulsions. This hypothesis was also verified by Evans and Wang⁴⁵ in a study on the distribution of small-scale energy depo-

sitions from low-LET particles in halocarbon R-115. d'Errico⁴⁴ reported their experimental data on the response of halocarbon R-115 and R-218 emulsions as a function of photon energy, expressed as bubbles per unit kerma in air along with the mass–energy absorption coefficients. For both emulsions, the measured air–kerma response follows the trend of the mass–energy absorption coefficient ratio, except below 30 keV where shielding by the glass vial and self-attenuation in the gel volume cause the decreasing measured response.

Superheated emulsion in heavy ions

It is known that superheated drops suspended in a viscoelastic gel are capable of detecting charged particles. The basic principle of detection is based on the hypothesis that a critical-radius spherical bubble must be reached in order to achieve bubble nucleation. The process of critical-radius bubble formation utilizes the energy deposited by the energetic particle in the liquid while passing through it, and when the deposited energy exceeds the critical energy required for liquid–vapour phase transformation, the drops nucleate. Although the utility of superheated emulsion as a neutron detector has already been established^{3,19,21,31}, investigations on its response to other energetic radiations are being pursued in various laboratories, including Bose Institute. Preliminary investigations on the application of superheated emulsion in proton detection and proton-beam dosimetry have been done by d'Errico and Egger⁴⁶. Responses of superheated liquid drops taken in the form of bubble detectors have been studied with high-energy Kr, Ar and N ions⁴⁷. Preliminary charged-particle detection results of Ing and Tomi⁴⁸ revealed that even when the LET of the charged particles themselves (α , ^{12}C and ^{19}F) did not permit them to be detected in a bubble detector, secondary particles from nuclear fragmentation interactions (induced by the ions) did create bubbles similar to irradiations with neutrons. Ing and Tomi⁴⁸ worked at HIMAC (Heavy Ion Medical Acceleration in Chiba) with different heavy ions like Kr, Ar and N. In an experiment with 400 MeV Kr ions, the temperature was fixed at 26°C and the reduced superheat was varied by changing the applied pressure on the bubble detector. In a second experiment, both Ar and N beams were used and the reduced superheat was varied by changing both the temperature and the applied pressure. Their result of LET of bubble formation against reduced superheat shows that if one knows the incident particle spectrum and computes the resulting LET distribution, it is possible to compute the bubble-detector response.

Recently in 2002, the Radiation Physics group of Bose Institute performed some preliminary experiments at VECC (Variable Energy Cyclotron Centre), Kolkata with 145 MeV Ne^{+6} ions and indigenously developed super-

heated emulsion. Recorded response shows an increase in nucleation rate with increase in flux of ions incident on the detector. Further work to study the response quantitatively is in progress.

1. Apfel, R. E., *Nucl. Instrum. Methods*, 1979, **162**, 603–608.
2. Ing, H. and Birnboim, H. C., *Nucl. Tracks Radiat. Meas.*, 1984, **8**, 285–288.
3. Knoll, G. F., *Radiation Detection and Measurement*, John Wiley, 1999, 3rd edn, p. 741.
4. Roy, S. C., *Radiat. Phys. Chem.*, 2001, **61**, 271–281.
5. Huang, K., *Statistical Mechanics*, 1975, chap. 2, p. 33.
6. Blander, M. and Katz, J. L., *AIChE J.*, 1975, **21**, 833–848.
7. Landau, L. D. and Lifshitz, E. M., *Statistical Physics*, 1985, 3rd edn, part-1, vol. 5, p. 533.
8. Maris, H. and Balibar, S., *Phys. Today*, 2000, pp. 29–34.
9. Gibbs, J. W., *Transl. Conn. Acad.*, 1875, **III**, 108.
10. Reid, R. C., *Adv. Chem. Eng.*, 1983, **12**, 183.
11. Das, Mala, Chatterjee, B. K., Roy, B. and Roy, S. C., *Phys. Rev. E*, 2000, **62**, 5843–5846.
12. Basu, D. K. and Sinha, D. B., *Indian J. Phys.*, 1968, **42**, 198–204.
13. Avedisian, C. T., *J. Phys. Chem. Ref. Data*, 1985, **14**, 695.
14. Glaser, D. A., *Phys. Rev.*, 1952, **87**, 665.
15. Seitz, F., *Phys. Fluids*, 1958, **1**, 2–13.
16. Bell, C. R., Oberle, N. P., Rohsenow, W., Todreas, N. and Tso, C., *Nucl. Sci. Eng.*, 1974, **53**, 458–465.
17. Sun, Y. Y., Chu, B. T. and Apfel, R. E., *J. Comput. Phys.*, 1992, **103**, 116–140.
18. Apfel, R. E., Roy, S. C. and Lo, Y. C., *Phys. Rev. A*, 1985, **31**, 3194–3198.
19. Apfel, R. E., *Nucl. Instrum. Methods*, 1981, **179**, 615.
20. Roy, S. C., Apfel, R. E. and Lo, Y. C., *Nucl. Instrum. Methods A*, 1987, **255**, 199–206.
21. Das, M., Roy, B., Chatterjee, B. K. and Roy, S. C., *Appl. Radiat. Isotope*, 2000, **53**, 759–763.
22. Apfel, R. E. and Roy, S. C., *Rev. Sci. Instrum.*, 1983, **54**, 1397–1400.
23. Roy, S. C., Roy, B., Das, M. and Chatterjee, B. K., Paper presented at the 4th IRRMA Conference, Rayleigh, North Carolina, 1999.
24. Apfel, R. E. and Roy, S. C., *Nucl. Instrum. Methods*, 1984, **219**, 582–587.
25. Apfel, R. E. and Roy, S. C., *Radiat. Prot. Dosim.*, 1985, **10**, 327–330.
26. Apfel, R. E., *Radiat. Prot. Dosim.*, 1992, **44**, 343.
27. Sawicki, J. A., *Nucl. Instrum. Methods A*, 1993, **336**, 215.
28. Vanhavere, F., Thierens, H. and Loos, M., *Radiat. Prot. Dosim.*, 1996, **65**, 425.
29. d’Errico, F., Nath, R., Tana, L., Curzio, G. and Alberts, W. G., *Med. Phys.*, 1998, **25**, 1717–1724.
30. Roy, S. C. and Sandison, G. A., *Med. Phys.*, 2000, **27**, 1800–1803.
31. d’Errico, F., Nath, R., Silvano, G. and Tana, L., *Int. J. Radiat. Oncol. Biol. Phys.*, 1998, **41**, 1185–1192.
32. Ing, H., Noulty, R. A. and McLean, T. D., *Radiat. Meas.*, 1997, **27**, 1–11.
33. d’Errico, F., Alberts, W. G., Curzio, G., Guldbakke, S., Kluge, H. and Matzke, M., *Radiat. Prot. Dosim.*, 1995, **61**, 159–162.
34. d’Errico, F., Alberts, W. G. and Matzke, M., *Radiat. Prot. Dosim.*, 1997, **70**, 103–108.
35. Das, M., Chatterjee, B. K., Roy, B. and Roy, S. C., *Nucl. Instrum. Methods A*, 2000, **452**, 273–279.
36. Das, M., Chatterjee, B. K., Roy, B. and Roy, S. C., *IRPS Bull.*, 1999, **13**, 3.
37. Das, M., Chatterjee, B. K., Roy, B. and Roy, S. C., *Radiat. Phys. Chem.*, 2001, **61**, 447–448.
38. Das, M., Roy, B., Chatterjee, B. K. and Roy, S. C., *Radiat. Phys. Chem.*, 2003 (in press).
39. d’Errico, F., *Radiat. Prot. Dosim.*, 1999, **84**, 55–62.
40. Apfel, R. E. and d’Errico, F., *Nucl. Instrum. Methods A*, 2002, **476**, 298–303.
41. d’Errico, F., Nath, R., Lamba, M. and Holland, S. K., *Phys. Med. Biol.*, 1998, **43**, 1147–1158.
42. Roy, B., Das, M., Roy, S. C. and Chatterjee, B. K., *Nucl. Instrum. Methods A*, 2000 **455**, 782–783.
43. Roy, B., Das, M., Roy, S. C. and Chatterjee, B. K., *Radiat. Phys. Chem.*, 2001, **61**, 509–510.
44. d’Errico, F., *Nucl. Instrum. Methods B*, 2001, **184**, 229–254.
45. Evans, T. M. and Wang, C. K. C., *Radiat. Res.*, 1999, **151**, 19–30.
46. d’Errico, F. and Egger, E., in *Hadrontherapy Oncology* (eds Amaldi, U. and Larsson, B.), Excerpta Medica, International Congress Series, Elsevier, Amsterdam, 1994, vol. 1077, pp. 488–494.
47. Ing, H. *et al.*, NIRS Report NIRS-HIMAC, NIRS-M-139 HIMAC-026, 1999, pp. 297–298.
48. Ing, H. and Tomi, L., Proceedings of the 2nd International Space Workshop, 2000, pp. 64–70.

ACKNOWLEDGEMENT. We acknowledge the partial financial support received from the Department of Science and Technology, Govt. of West Bengal.

Received 10 May 2002; revised accepted 20 December 2002